KRYSTIAN NOWAKOWSKI, ARTUR PEREK,
MAREK IZDEBSKI, RAFAŁ LEDZION, PIOTR GÓRSKI

Institute of Physics, Lodz University of Technology
ul. Wólczańska 219, 90-924 Łódź, Poland,
e-mail: izdebski@p.lodz.pl

OPTIMIZATION OF MEASUREMENT CONDITIONS OF KERR CONSTANT IN OPTICALLY ACTIVE LIQUIDS ON THE EXAMPLE OF CASTOR OIL

The results of measurements of Kerr constant in castor oil, obtained by dynamic-polarimetric method are presented. Variable optical path length and four measurement setup configurations were used. They differed by the orientation of polarizer and of quarter-wave plate and therefore they were non-equivalent when other, unwanted effects occurred. It was shown that the Kerr constant measurement performed with use of only one system configuration and one length of optical path may be strongly affected by other effects, however taking the arithmetic mean of two results obtained from appropriate system configurations significantly reduces this error. Theoretical dependences were fitted to the experimental results, which allowed for approximation of other constants, like dichroism, linear birefringence and optical activity induced by external electric field (electrogyration).

Keywords: castor oil, optical polarimetric technique, quadratic electro-optic effect, optical activity, dichroism.

1. INTRODUCTION

Castor oil is a non-edible, light-yellow, transparent and viscous liquid, obtained from the seeds of castor oil plant. It has been used since ancient times in Egypt during mummification and worldwide in traditional medicine [1]. Nowadays it plays an important role in industry, having various applications, including production of paints, food, plastics, medicines, cosmetics, biofuels and many others [1,2]. Its main components are triglycerides of fatty acids, mainly ricinoleic acid (over 89%), linoleic acid (ca. 4%) and oleic acid (ca. 3%) [2]. Although castor oil is considered to be relatively stable, its low oxidative and

temperature stability limits its widespread use. Recently it has been shown, that there is a clear relationship between aging of medical castor oil and its temperature and frequency dependence of the Kerr constant, which is a fact that could be used in continuous quality control systems [3]. However, the cited research on castor oil ageing assumed that it has internal symmetry described by $\infty\infty m$ Curie group, which was later shown to be not the case. In fact, when the oil is enclosed between two, closely spaced, plane-parallel metal electrodes, the internal symmetry is described by $\infty 2$ Curie group [4]. When this lesser symmetry is taken into account, the equations describing Kerr effect and light propagation in castor oil become highly complicated, therefore some assumptions, e.g. lack of dichroism, are usually made to simplify the formulas. Therefore, in order to obtain precise and reliable results, we should carefully consider several other unwanted effects that occur simultaneously during the measurement and may significantly affect the outcome. The effects that should be taken into account are: the natural optical activity [4], the optical activity induced by applied electric field (called the electrogyration effect) [5] and the effects resulting from the interaction of the oil with plane-parallel electrodes immersed in it, such as dichroism and weak linear birefringence with the optical axis perpendicular to the plane of the electrodes [4,6]. The numerical analysis recently presented in Ref. [7] has shown, that the measurement of Kerr effect in castor oil is sensitive to the influence of natural optical activity, linear birefringence, and dichroism, while the electrogyration is less important. According to the numerical simulations performed for medical castor oil, a measurement error is ca. 22% for optical path length of 10 cm. In the same work it was deduced, that there should be two pairs of the possible arrangements of the measurement system, which would result in such errors due to simplifications, that are equal in magnitude, but opposite in sign. Taking the average of these two results would eliminate the error introduced due to simplifications. The aim of this research is to check experimentally the theoretical predictions described above and to formulate practical conclusions concerning the optimal conditions for measuring the Kerr constant.

2. MATHEMATICAL MODEL OF MEASUREMENT

Our earlier observations showed that castor oil between a pair of metal plane-parallel electrodes has an internal symmetry described by $\infty 2$ Curie group with the optical axis directed perpendicularly to the plane of the electrodes [4]. In this situation the only possible form of the vector of applied electric field written in the principal axes system *XYZ* is $\mathbf{E} = (0, 0, E)$. Let us consider the light beam propagating in the direction $\mathbf{s} = [1, 0, 0]$. The total complex

impermeability tensor [*B*] for this configuration written in the *XYZ* coordinates with the accuracy to the terms proportional to *E* has the following form [7]:

$$[B] = \begin{bmatrix} n_{01}^{-2} + q_{13}E^2 & 0 & 0 \\ 0 & n_{01}^{-2} + q_{13}E^2 & B_{23} \\ 0 & -B_{23} & n_{03}^{-2} + q_{33}E^2 \end{bmatrix}, \tag{1}$$

$$B_{23} = i\left[n_{01}^{-2} n_{03}^{-2} \left(g_{11}^{(0)} + \beta_{13}E^2 \right) + g_{11}^{(0)} \left(n_{01}^{-2} q_{33} + n_{03}^{-2} q_{13} \right) E^2 \right], \tag{2}$$

where n_{01} and n_{03} are the principal refractive indices, $g_{ii}^{(0)}$ are the components of natural optical activity tensor, q_{ij} are the components of the quadratic electro-optic tensor, and β_{13} is the component of the quadratic electrogyration tensor (the forms of the tensors can be found, e.g., in Refs. [5,7,8]). It is worth noting that the terms in Eq. (2) containing the products of $g_{11}^{(0)}$ (of the order of 10^{-7}) and q_{ij} are negligible and the term $n_{01}^{-2} n_{03}^{-2}$ is very close to n_0^{-4}, where $n_0 = (n_{01} + n_{03})/2$ is the average refractive index.

Let us introduce another coordinate system, *X'Y'Z'*, related to the experimental setup in which the +*Z'* axis is along the light beam **s'** = [0, 0, 1] and the +*X'* axis defines the reference zero azimuth. A typical experimental setup for measurements of electro-optic coefficients based on the optical polarimetric method consists of a linear polarizer of the azimuth $\alpha_P = \pm 45°$ (relative to +*X'* axis), a cuvette with the oil and immersed electrodes, a quarter-wave plate of the azimuth $\alpha_Q = 0°$ or 90° for the fast wave, and a linear analyzer of any arbitrary azimuth α_A. The intensity *I* of the light passing through this system relative to the intensity I_p behind the polarizer has been derived previously employing Jones calculus [7]:

$$\begin{aligned} \frac{I}{I_p} = {}& \tfrac{1}{4}\left(T_f^2 + T_s^2 \right) + \\ & + \tfrac{1}{4}\left(T_f^2 - T_s^2 \right) \frac{(B_{11}' - B_{22}')\cos(2\alpha_a) - 2z\,\mathrm{Im}[B_{12}']\sin(2\alpha_A)}{\sqrt{(B_{11}' - B_{22}')^2 + 4B_{12}'B_{12}'^{*}}} + \\ & \mp \cos(2\alpha_A) T_f T_s \frac{\mathrm{Im}[B_{12}']}{\sqrt{(B_{11}' - B_{22}')^2 + 4B_{12}'B_{12}'^{*}}}\sin\Gamma + \\ & \mp z\,\tfrac{1}{2}\sin(2\alpha_A) T_f T_s \frac{B_{11}' - B_{22}'}{\sqrt{(B_{11}' - B_{22}')^2 + 4B_{12}'B_{12}'^{*}}}\sin\Gamma, \end{aligned} \tag{3}$$

where the symbol * indicates the complex conjugate, the upper signs in the "$\mp$" symbol correspond to $\alpha_P = +45°$ and the lower signs to $\alpha_P = -45°$, $z = +1$ for $\alpha_Q = 0°$ and $z = -1$ for $90°$, T_f and T_s are the amplitude transmission coefficients for the fast and slow waves, respectively, and Γ is the phase difference between the slow and fast waves

$$\Gamma = \frac{2\pi L}{\lambda}(n_s - n_f) . \tag{4}$$

In Eq. (4) λ is the wavelength of the light, L is the light path length between electrodes in the cuvette, and n_f and n_s are the refractive indices of the fast and slow waves, respectively. In the general case, calculation of Γ is a bit more complicated, however, when the relation $B'_{11} + B'_{22} >> \sqrt{(B'_{11} - B'_{22})^2 + 4B'_{12}B'^*_{12}}$ is satisfied and n_{01} and n_{03} have very similar values, we can calculate Γ as [5,7]:

$$\Gamma \approx \frac{2\sqrt{2}\,\pi L}{\lambda}\,\frac{\sqrt{(B'_{11} - B'_{22})^2 + 4B'_{12}B'^*_{12}}}{(B'_{11} + B'_{22})^{3/2}} \approx \frac{\pi L n_0^3}{\lambda}\sqrt{(B'_{11} - B'_{22})^2 + 4B'_{12}B'^*_{12}} . \tag{5}$$

The matrix of transformation from the *XYZ* to *X'Y'Z'* coordinates can be chosen for example as follows:

$$[\mathbf{a}] = \begin{bmatrix} 0 & 0 & -1 \\ 0 & 1 & 0 \\ 1 & 0 & 0 \end{bmatrix}. \tag{6}$$

Hence, the selected components of the impermeability tensor $[B'] = [\mathbf{a}][B][\mathbf{a}]^T$ written in the *X'Y'Z'* coordinates are:

$$B'_{22} - B'_{11} = n_{01}^{-2} - n_{03}^{-2} + (q_{13} - q_{33})E^2 , \tag{7}$$

$$B'_{12} = B_{23} \approx i\,n_0^{-4}g_{11}^{(0)} + i\,n_0^{-4}\beta_{13}E^2 . \tag{8}$$

The transmissions T_f and T_s in Eqs. (3) depend on the path length L according to Bouguer's law:

$$T_f^2 = \exp(-\kappa_f L) , \quad T_s^2 = \exp(-\kappa_s L), \tag{9}$$

where κ_f and κ_s [1/m] are the length-independent absorption coefficients. The difference $\kappa_f - \kappa_s$ is related with the relative difference D in transmissions:

$$D(L) = (T_f - T_s)/\overline{T} = 2\tanh\!\left[-0.25(\kappa_f - \kappa_s)L\right], \tag{10}$$

where $\overline{T} = (T_f + T_s)/2$ is the average transmission coefficient. The relationship (10) allows to calculate $D(L)$ for any path length L when the value of D is given for any fixed length. The other expressions in Eq. (3), which depend on the transmission coefficients, can be calculated as follows:

$$T_{\mathrm{f}}^2 + T_{\mathrm{s}}^2 = 2\bar{T}^2\left(1 + 0.25D^2\right), \tag{11}$$

$$T_{\mathrm{f}}^2 - T_{\mathrm{s}}^2 = 2\bar{T}^2 D^2, \tag{12}$$

$$T_{\mathrm{f}}T_{\mathrm{s}} = \bar{T}^2\left(1 - 0.25D^2\right). \tag{13}$$

Since all the expressions in Eq. (3) are proportional to $\bar{T}^2$ this variable reduces in calculations of modulation index related to the changes in the intensity I due to an applied electric field E.

3. EXPERIMENTAL

3.1. Method

The dynamic-polarized method is based on measuring the intensity of light passing through Kerr cell placed between crossed polarizers. Across the Kerr cell, a sinusoidal alternating electric field of frequency 417 Hz was applied. As the Kerr effect depends here on the square of the electric field, the change in optical properties of the medium was modulated with the frequency equal to the second harmonics of the field frequency, since the Kerr effect is the same for both directions of the field. Two components of the emerging light were measured, the constant component I_0 and the component at the second harmonics of the modulating field $I_{2\omega}$. Calculating the ratio of these two quantities, we get modulation index $m_{2\omega}$ defined as $m_{2\omega} = I_{2\omega}/I_0$. Since we were using a photodiode to measure light intensity, it is also possible to express $m_{2\omega}$ as a function of the amplitudes of signals given by the photodiode, rather than light intensities:

$$m_{2\omega} = \frac{I_{2\omega}}{I_0} = \frac{U_{2\omega}}{U_0}, \tag{14}$$

where $U_{2\omega}$ is the RMS voltage of the signal from photodiode at the second harmonics of the applied field frequency and U_0 is the constant component of the signal from photodiode. To the best of our knowledge, all the previous research in this matter assumed that the modulation index $m_{2\omega}$ is a linear function of the square of applied voltage (or electric field), i.e.:

$$m_{2\omega} = a\,U_{\mathrm{m}}^2 + b, \tag{15}$$

where U_{m} is the RMS voltage applied to the electrodes and a is the slope. This assumption holds true if the simplifications mentioned in the introduction are valid. If this relation is indeed linear, then it is possible to calculate the Kerr coefficient K of the material using the following formula:

$$K = \frac{a\,d^2}{\sqrt{2}\,\pi L}, \tag{16}$$

where d is the distance between the electrodes and L is the optical path length.

3.2. Setup

The Kerr cell was a glass cuvette with stainless steel electrodes immersed in castor oil. A separator made of polycarbonate fixed electrodes in positions. The cross-section of this setup is presented in Fig. 1.
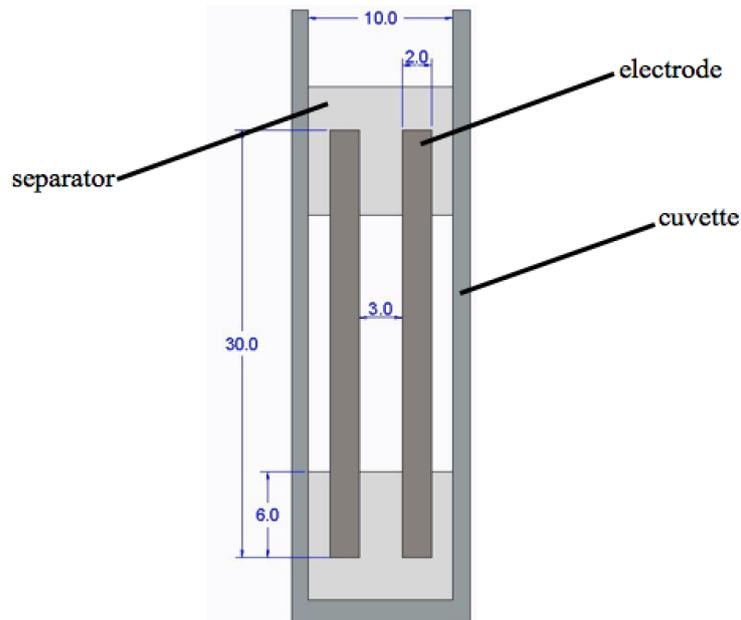
Fig. 1. Cross-section of the experimental Kerr cell

The length of electrodes was 99 ± 0.1 mm and 49 ± 0.1 mm. The light beam was directed perpendicularly to the applied electric field. The distance d between the electrodes was 3 ± 0.02 mm. The optical path length was increased by adding more cuvettes and connecting electrodes in series, with the step of 4.9 cm. Thus, there was 2 mm of glass between adjacent electrodes, as the cuvettes' walls are 1 mm thick. Nevertheless this system was assumed to be one uniform Kerr cell of greater length. The oil under investigation was Sigma-Aldrich castor oil number 259853 (batch number MKBL5196). The oil was poured into cuvettes

10 days before the first measurement, to allow little air bubbles to escape, as castor oil is dense and highly viscous. The measurements were carried out for another 13 days, so altogether the oil spent 23 days in cuvettes, all the time open to air and in stable temperature of 20-22°C. The complete measurement system is presented schematically in Fig. 2.
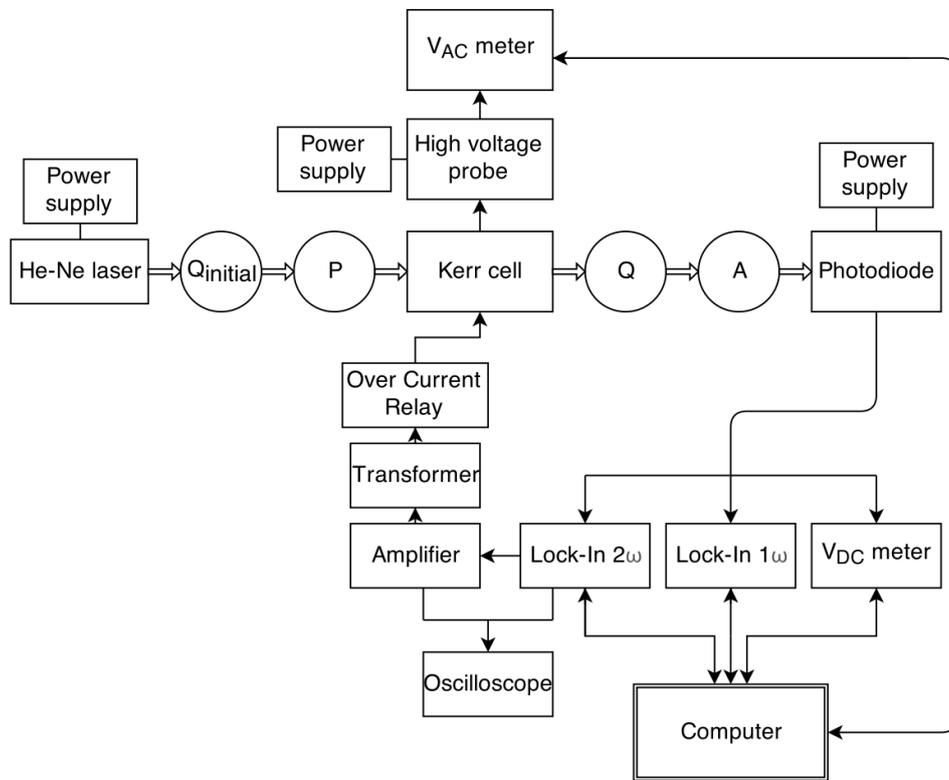
Fig. 2. Scheme of the measurement system

The light source was a He-Ne laser of wavelength $\lambda = 632.8$ nm. Letters Q, P and A stand for quarter-wave plate, polarizer and analyzer, respectively. An additional $Q_{initial}$ quarter-wave plate placed between the laser and the polarizer was oriented in such a way that it changed the polarization of light to circular. The RMS of voltage applied to the electrodes in the Kerr cell was measured by Keithley multimeter 2000 through Tektronix P6015 high voltage probe. The intensity of light behind the analyzer was measured by Thorlabs photodiode PDA100A-EC. Three components of that signal were recorded. The DC

component was measured by Keithley multimeter 2700, the RMS of components at the first and at the second harmonic of modulating field were measured by digital signal processing lock-in amplifiers produced by EG&G instruments, model 7265. One of the lock-in amplifiers was also used for generating the modulating signal, that was later amplified and passed through a transformer in order to obtain voltages up to 3 kV. An over-current relay was added after the transformer for safety. A computer program controlled the measurement process and data acquisition.

3.3. Procedure

According to the theoretical analysis in Ref. [7], the settings giving desired series of results, that have errors equal in magnitude but opposite in sign, differ from each other only by the rotation of quarter-wave plate Q by 90°. Turning the polarizer P by 90° allows to obtain a different pair of series. The reference direction, that we will use to describe the orientation of optical elements, is the normal to the electrode surfaces. The angle 0° means direction perpendicular to the electrode surfaces and angle 90° means direction tangent to these surfaces. The orientation of the optical axis of the analyzer A was constant throughout the experiment, and equal to −45°. Shorthand notation of this orientation will be $\alpha_A = -45°$. The polarizer and quarter-wave plate orientation will be described in the same way as α_P and α_Q. When it comes to the quarter-wave plate Q, its position will be described by two arbitrary numbers, −1 and 1. One of them means that the extraordinary axis is perpendicular to the electrode surfaces and the other means that it is parallel to them. We have no way to recognize which one is which; nevertheless, the measurement was done for both orientations. The experimental procedure was as follows:

1.   Set $\alpha_A = -45°$ and $\alpha_P = 45°$ (polarizer and analyzer crossed).
2.   Insert the first Kerr cell of length 4.9 cm to the system.
3.   Set $\alpha_Q = 1$.
4.   Measure the Kerr effect for a given voltage range.
5.   Turn Q by 90°, i.e. set $\alpha_Q = -1$.
6.   Measure the Kerr effect for a given voltage range again.
7.   Increase the length of the Kerr cell by inserting next cuvette.
8.   Repeat steps 3-7 until achieving the maximal length ($L = 79.2$ cm).
9.   Set $\alpha_P = -45°$ (optical axes of polarizer and analyzer are parallel).
10. Repeat steps 3-7, this time decreasing the path length by removing cuvettes.

The voltages applied to the electrodes were not exactly the same for every path length, as adding more cuvettes increased the capacitance of the system, resulting in lower field strength across the Kerr cell for the same signal generated by Lock-in amplifier. The program took 10 measurements at each voltage value, in the range of ca. 350-2000 V, with the step of ca. 70 V.

4. RESULTS

First of all, according to Eq. (14), the modulation index $m_{2\omega}$ was calculated and then plotted against the square of the RMS of voltage applied to the electrodes, U_{m}^2. Then a linear function was fitted to the data points and its slope a, needed to calculate the Kerr constant according to Eq. (16), was get. Some exemplary results are plotted in Fig. 3, for easier comparison, for $m_{2\omega}/L$ as a function of the square of the electric field intensity E^2.
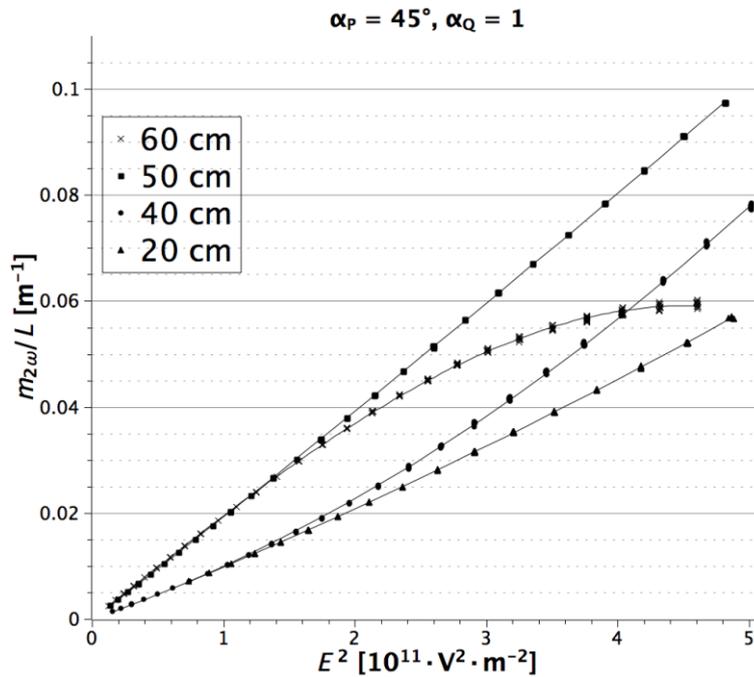
Fig. 3. The experimental dependence of the ratio of modulation index to path length, $m_{2\omega}/L$, on the square of electric field intensity E^2 for SIGMA ALDRICH castor oil at room temperature and field frequency 417 Hz for crossed polarizer and analyzer

As it can be seen, not only are the relationships non-linear, but also they tend to change their general shape, e.g. the curve for 40 cm is parabolic, curve for 50 cm becomes more linear again, while the curve 60 cm has exponential-like shape. Because of this nonlinearity, Eq. (16) was not used to find the Kerr constant K for the optical path lengths over 50 cm. For the same reason, only the linear part of the above plot was used for fitting for $L = 40$ cm. The values of Kerr constant K, obtained from Eq. (16), are plotted below, as a function of L:

K(L) – experimental dependance
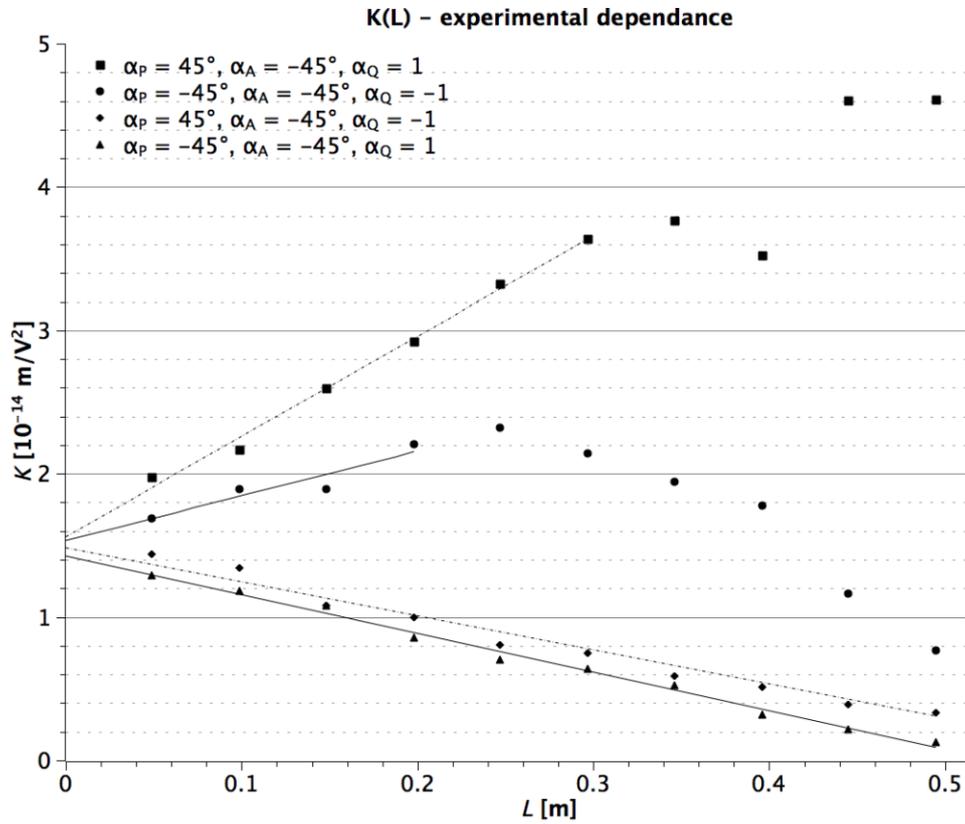
Fig. 4. The experimental dependences of the Kerr constant K on the path length L obtained for SIGMA-ALDRICH castor oil at room temperature and frequency 417 Hz for the four combinations of the polarizer and quarter-wave azimuths

The experimental dependence of K on L was used to match the constants $n_{01} - n_{03}$, β_{13}, and $(T_f - T_s)/\overline{T}$ for $L = 10$ cm, which are present in the theoretical

relationships given in Chapter 2. Furthermore, we used the following fixed constants, which are known in advance from various measurements:

- $n_0 = 1.48$ [5],
- the Kerr constant $K = 1.5 \cdot 10^{-14}$ mV^{-2} obtained in this work by extrapolating the experimental $K(L)$ dependences for $L \to 0$, which allows to calculate the effective coefficient of the quadratic electro-optic effect $|q_{33} - q_{13}| = 2\lambda K/n_0^3 \approx 5.8 \cdot 10^{-21}$ m^{2}V^{-2},
- the angle $\phi = -3.5°$ of turning of the polarization plane in the oil obtained in this work for $L = 10$ cm and $\alpha_P = 0$, which allows to calculate $g_{11}^{(0)} = -1.82 \cdot 10^{-7}$ according to the formula $g_{11}^{(0)} = \lambda n_0 \phi/(\pi L)$ derived in Ref. [5].

The lock-in amplifier was simulated numerically by computing the coefficients in the following Fourier series:

$$\frac{I}{I_p} = \frac{I_0}{I_p} + \frac{I_\omega}{I_p}\sin(\omega t + \varphi_1) + \frac{I_{2\omega}}{I_p}\sin(2\omega t + \varphi_2) + \dots, \tag{17}$$

for I/I_p given by Eq. (3) with substituted equations (5), (7), (8) and (10)-(13). Then, the coefficients of this series were used to calculate the modulation index:

$$m_{2\omega} = \frac{I_{2\omega}/I_p}{I_0/I_p}. \tag{18}$$

Since the dependence of $m_{2\omega}$ on U_m^2 may differ from the linear function in Eq. (15), our calculations were performed for various U_m voltages and the average slope a was matched. Then, the Kerr constant was calculated like for the experimental data, employing Eq. (16).

The numerically obtained $K(L)$ dependences shown in Fig. 5 are roughly in line with all four experimental series in Fig. 4 when the following constants are substituted:

$$|T_f - T_s|/\overline{T} = 0.034 \text{ for the path length } L = 0.1 \text{ m}, \tag{19}$$

$$|n_{01} - n_{03}| = 2.5 \cdot 10^{-7}, \tag{20}$$

$$|\beta_{13}| = 1.0 \cdot 10^{-20} \text{ m}^2\text{V}^{-2}. \tag{21}$$

Although the signs of $T_f - T_s$, $n_{01} - n_{03}$, β_{13} and $q_{33} - q_{13}$ can not be completely arbitrary, some combinations of the signs lead to similar results and we can not unambiguously determine the signs of individual constants.

$K(L)$ - theoretical dependence
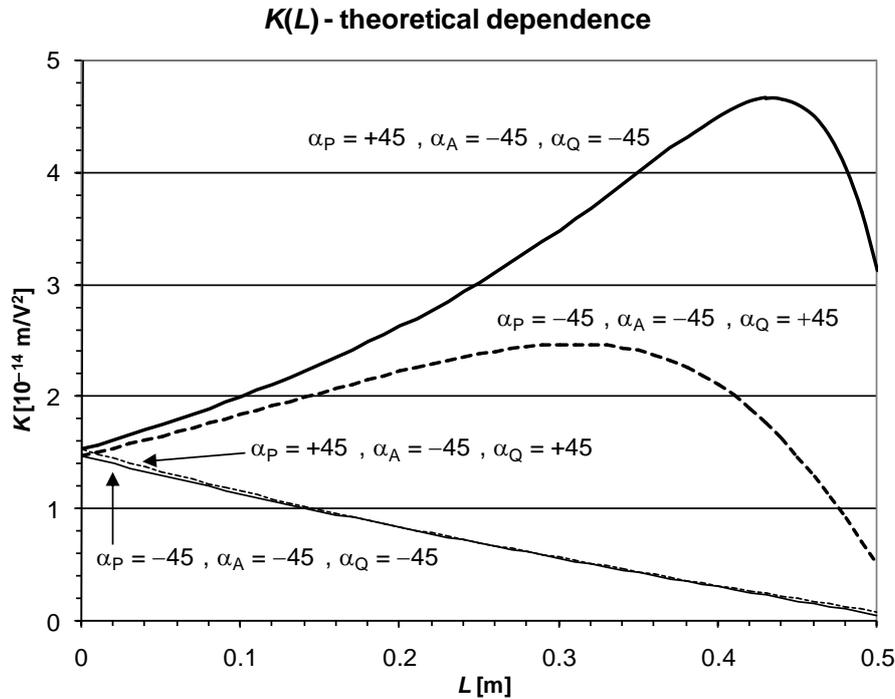
Fig. 5. The theoretical dependences of the Kerr constant K on the path length L obtained for $(T_f - T_s)/T = -0.034$ for path length 0.1 m, $n_{01} - n_{03} = 2.5 \cdot 10^{-7}$, $q_{33} - q_{13} = 5.8 \cdot 10^{-21}$ m^{2}V^{-2} and $\beta_{13} = -1.0 \cdot 10^{-20}$ m^{2}V^{-2}

It is worth noting that to obtain a satisfactory agreement between the theoretical and experimental dependences, we cannot neglect any of the effects such as the linear birefringence, the dichroism, the natural optical activity and the quadratic electrogyration effect.

5. CONCLUSIONS

Our experimental results obtained for pure castor oil for research purposes confirm the existence of the effects observed previously in other experimental systems, such as the linear birefringence [4,6], the dichroism [4,6], the natural optical activity [4], and the optical activity induced by an applied electric field (electrogyration effect) [5], which are not taken into account in the simplified formula (16) typically applied to processing of experimental data. It is possible to derive the exact formula, which takes into account all of the phenomena mentioned. However, in practice the use of such formula would be very

problematic because of its complexity and dependence on a number of coefficients that require measurements in other experimental setups. Moreover, some of these coefficients are likely to be unstable and sensitive to many factors such as the oil purity, ageing processes, temperature, the history of the applied electric field including many hours before the measurement and others. In this situation, our goal is to find such a way of determining the Kerr constant that allows for reducing the influence of unwanted effects, so it is not necessary to measure them beforehand.

Our new experimental results and numerical analysis confirms the conclusion reached previously in Ref. [7] that the contribution of undesirable effects can be substantially reduced by calculating the arithmetic mean of the two values of Kerr constant calculated according to the formula (16) for the two measurements differing in the orientation of the quarter-wave plate. However, this conclusion requires the addition of a new assumption that these two measurements should be carried out for a parallel orientation of the analyzer to polarizer. The measurements performed in traditional configuration with crossed polarizers and various orientations of quarter-wave plate do not ensure as good reduction of errors in the arithmetic mean.

The values of the linear birefringence and dichroism estimated in this work are in good agreement with the results obtained previously for medical castor oil [4]. The value of the dichroism $|T_f - T_s|/\overline{T} = 1.0 \cdot 10^{-2}$ (for $L = 10$ cm) obtained recently in Ref. [5] is significantly smaller, but this results probably from instability of this coefficient rather than from erroneous measurement method.

The absolute value of the electrogyration coefficient $|\beta_{13}| = 1.0 \cdot 10^{-20}$ m^{2}V^{-2} estimated roughly in this work is much higher than the value $1.4 \cdot 10^{-22}$ m^{2}V^{-2} obtained previously in another measurement system [5]. According to our best knowledge there are no other published results for liquids, and we can only conclude that both values are in the range of values $10^{-22} \ldots 10^{-18}$ known from the literature for solid crystals at room temperature [9]. At the present stage of research we cannot decide whether one of the results is erroneous, because it is possible that we are dealing with a coefficient that is unstable.

REFERENCES

[1] **Khan I.A., Abourashed E.A.,** Leung's Encyclopedia of Common Natural Ingredients Used in Food, Drugs and Cosmetics, John Wiley & Sons, Inc., 2010.
[2] **Ogunniyi D.S.,** Bioresource Technology **97(9)** (2006) 1086.
[3] **Stępień M., Ledzion R., Górski P., Kucharczyk W.,** Sci. Bull. Lodz Univ. Tech., s. Physics, **33** (2012) 89.

[4] **Izdebski M., Ledzion R., Górski P.,** Sci. Bull. Lodz Univ. Tech., s. Physics, **33** (2012) 39.

[5] **Izdebski M., Ledzion R., Górski P.,** "Measurement of quadratic electrogyration effect in castor oil", in review in Optics Communications.

[6] **Izdebski M., Ledzion R.,** "New method for measurement of very weak linear birefringence and dichroism in liquids on the example of castor oil between metal electrodes", this volume.

[7] **Izdebski M., Ledzion R., Kucharczyk W.,** Sci. Bull. Lodz Univ. Tech., s. Physics, **34** (2013) 5.

[8] **Sirotin Yu.I., Shaskolskaya M.P.,** Fundamentals of crystal physics, Mir Publishers, 1982.

[9] **Bhalla A.S., Cook W.R., Hearmon R.F.S., Jerphagnon J., Kurtz S.K., Liu S.T., Nelson D.F., Oudar J.-L.,** Crystal and solid state physics, in: Hellwege K.-H., Hellwege A. (Eds.), Landolt-Börnstein Numerical Data and Functional Relationships in Science and Technology, **Vol. 18** of New Series, Group III, Springer, Berlin, 1984, pp. 431-434.

OPTYMALIZACJA WARUNKÓW POMIARU STAŁEJ KERRA W CIECZACH AKTYWNYCH OPTYCZNIE NA PRZYKŁADZIE OLEJU RYCYNOWEGO

Streszczenie

Przedstawiono wyniki pomiarów stałej Kerra w oleju rycynowym metodą polaryzacyjno-optyczną dla różnych długości drogi światła w próbce przy czterech konfiguracjach pomiarowych, nierównoważnych pod względem wpływu innych niepożądanych efektów, które różnią się orientacjami polaryzatora i płytki ćwierćfalowej. Pokazano, że pomiar stałej Kerra przeprowadzony dla tylko jednej konfiguracji pomiarowej przy jednej długości drogi światła w próbce może być obciążony znacznym wkładem kilku innych niepożądanych efektów, jednakże obliczenie średniej arytmetycznej z pomiarów w dwóch odpowiednio dobranych konfiguracjach pomiarowych pozwala na znaczne zredukowanie błędów pomiarowych. Do wyników doświadczalnych dopasowano zależności teoretyczne, co oprócz pomiaru stałej Kerra pozwoliło także na zgrubne oszacowanie innych wielkości takich jak dichroizm, liniowa dwójłomność i aktywność optyczna indukowana polem elektrycznym (elektrożyracja).